URN (Paper): urn:nbn:de:gbv:ilm1-2011iwk-107:2

56TH INTERNATIONAL SCIENTIFIC COLLOQUIUM
Ilmenau University of Technology, 12 – 16 September 2011
URN: urn:nbn:gbv:ilm1-2011iwk:5

EXPERIMENTAL INVESTIGATION OF LIQUID FLOWS IN DIFFERENT PIPE CONFIGURATIONS USING IMPROVED LDA TECHNIQUES

Gudrun Wendt

Physikalisch-Technische Bundesanstalt Braunschweig, Germany

ABSTRACT

Improved experimental setups and actual results of three-dimensional velocity measurements in liquid flows using Laser-Doppler-Anemometry (LDA) are described in this paper. Investigations are carried out inside pipes of circular cross section at different flow rates under different disturbed and undisturbed flow conditions. Corresponding technical solutions as well as the optimized LDA data processing and presentation are explained.

In a second step, the LDA hard- and software is modified to be employable for a special application – the measurement of velocity distributions inside a multi-jet water meter. The goal is to study the influence of different flow conditions at the inlet of the meter on the meter's metrological behavior.

Beside qualitative descriptions of flow patterns by various 2D- and 3D-diagrams, dimensionless parameters are defined to realize a quantitative characterization of the flows investigated.

Index Terms **–** Laser Doppler Anemometer, 3D-velocity distributions, pipe flow, flow disturbances, swirl generator, installation effects, multi-jet water meter

1. METROLOGICAL BACKGROUND

Nearly all types of flowrate measuring devices (flow meters) are affected by the flow conditions at their inlet section. So-called disturbed velocity distributions of non-regular shape, with asymmetries or swirls can lead to meter errors in unpredictable high order up to ten percent or more [1,2]. In the last years, great effort has been made to find suitable methods to investigate the actual flow behavior and to realize a close look into the flow under several conditions and pipe configurations; for example behind disturbances, at the meter's inlet or inside the meter itself. The results should form the base of a theoretical model which allows an explanation and – if possible – a prediction of the changes in the corresponding flow meter indications observed. The focus was mainly directed to non-intrusive optical methods and to water as the measuring fluid.

2. TECHNICAL SOLUTION

As a result of successful cooperation between the Physikalisch-Technische Bundesanstalt (PTB) and two small spin-off enterprises (ILA Inc. Germany, OPTOLUTION Inc. Switzerland), an automated modular laser system has been developed allowing measurements of three-dimensional velocity distributions in liquid pipe flows. The system comprises a traversable Laser-Doppler-Anemometer (LDA) consisting of a Nd:YAG laser and related optics, an universally adaptable window chamber, and a special software [3].

The LDA technique is a contactless optical method to measure the local velocity of a flowing fluid with high temporal and spatial resolution. In the present case, the individual measuring positions inside the pipe can be freely selected in advance and in any order. A special laserbeam-backtracking software calculates and activates the necessary traveling of the LDA unit taking into account all changes of the laser beam due to refractive effects at the transit surfaces from air to glass and water. Fig. 1 shows the experimental set-up with a standard window chamber adapted to a 25 mm straight pipe. In the lower right corner the head of the traversable LDA unit is seen. Detailed information about the LDA method and the measuring system developed is given in [4].

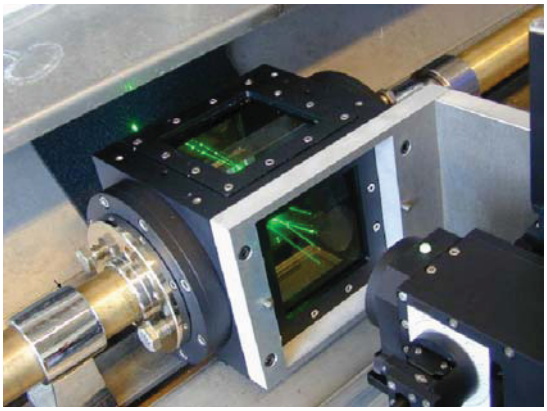

Figure 1: Experimental set-up of a 25 mm pipe configuration with window chamber and the traversable LDA unit

The window chamber enables the optical access to the pipe section under investigation. Its special design and the modular structure (see Fig. 2) offers a high variability to ensure an optimum adaptation to the respective measuring situation. The outer connecting flanges, the inner glass tube and its adapter can be flexibly configured, so they will provide exact fitting to the surrounding pipe work. That way, additional influences of the window chamber on the flow under test are minimized. The main body is water filled. The critical transit of the laser beams from air to glass and water takes place on the surface of a plane-parallel glass plate. This altogether essentially reduces possible refraction effects and guarantees a proper work of the laserbeam-backtracking system.

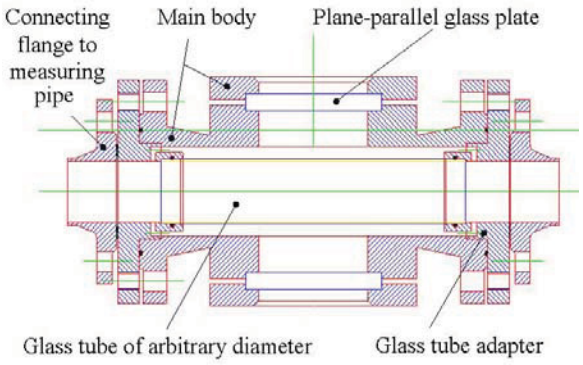

Figure 2: Construction details of the window chamber

The laser Doppler anemometry is a punctual method. It gives the local flow velocity only within the point of intersection of the laser beams and only for the velocity component perpendicular to the crossing plane of the beams.

To get information about the complete three-dimensional velocity distribution over the whole pipe cross section, two separate work steps have to be carried out:

- Depending on the desired resolution of the velocity field under investigation (i.e. on the density of the individual measuring points across the pipe cross section), the LDA unit should be moved successively from one measuring position to the next. Fig. 3 shows the grid tailored for the current investigation. It consists of altogether 301 individual measuring points located along 15 concentric circles around the centre point with an angular distance of 18° each. Regarding the higher velocity gradient expected towards the pipe wall, the density of points is increased in this region.
- The measurement of all three components of each velocity vector needs three different orientations of the laser unit. In the present case this is achieved by using the LDA unit horizontally in two orientations where only its head is rotated by 90°. Afterwards the complete laser unit is moved to an upright position to get the third component.

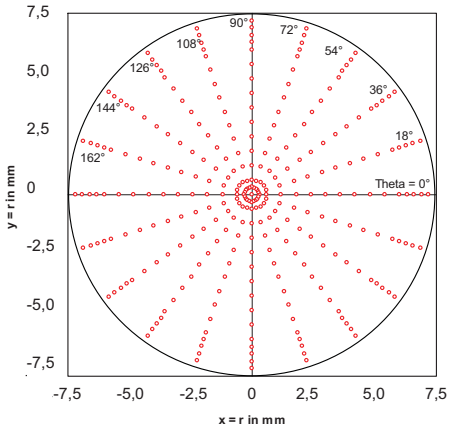

Figure 3: Measuring grid for a circular pipe cross section with a diameter of d=15 mm

After completing all measurements, the data of each measuring point are merged and prepared for further interpretation and evaluation. The related software gives several options to present the measuring results, for example, in form of:

- Spatial diagrams of the *axial velocity distribution* in m/s or normalized to the mean volumetric velocity $w_{vol} = Q_V/(\pi \cdot R^2)$.
  (Look at Fig. 4 for an undisturbed turbulent flow after a long straight pipe)
- Diagrams of the *tangential velocity distribution* where the lengths of the arrows are normalized to the mean volumetric (axial) velocity, the colours represent the belonging swirl angles.
  (Look at Fig. 5 for a swirl afflicted flow behind a swirl generator)
- Diagrams of the *degree of turbulence* in %.
  (Look at Fig. 6 for an undisturbed flow)
- Single *velocity profiles* and degrees of turbulence along each diameter of the measuring grid.
  (Look at Fig. 7 for an asymmetric flow behind a swirl generator)

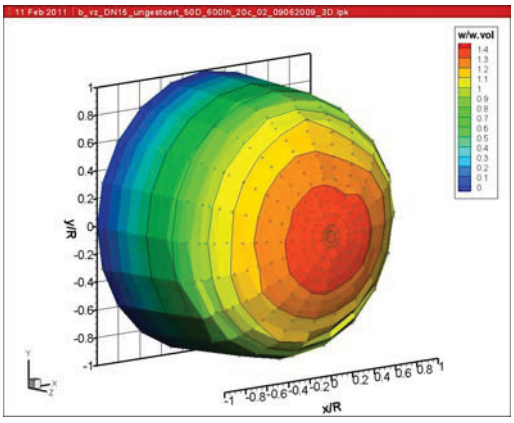

Figure 4: Normalized axial velocity distribution for an undisturbed turbulent flow;
Pipe diameter d=15 mm, length of the straight inlet pipe 50 d, flowrate 600 l/h

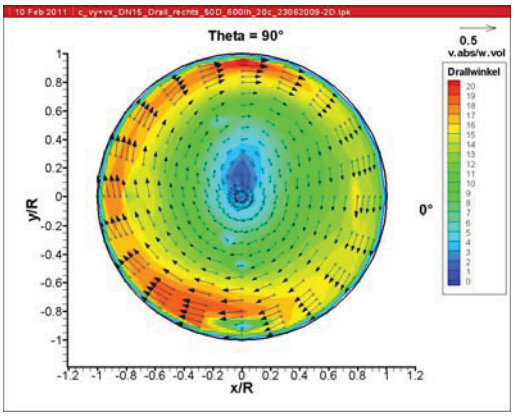

Figure 5: Normalized tangential velocity distribution for a swirl afflicted flow behind a swirl generator; Pipe diameter d=15 mm, distance between swirl generator and measuring section 5 d, flowrate 600 l/h

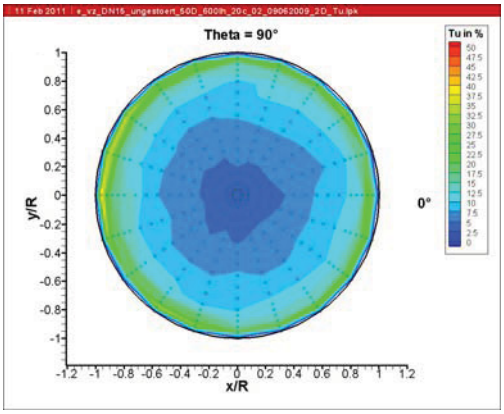

Figure 6: Percentage degree of turbulence Tu; Pipe diameter d=15 mm, length of the straight inlet pipe 50 d, flowrate 1.200 l/h

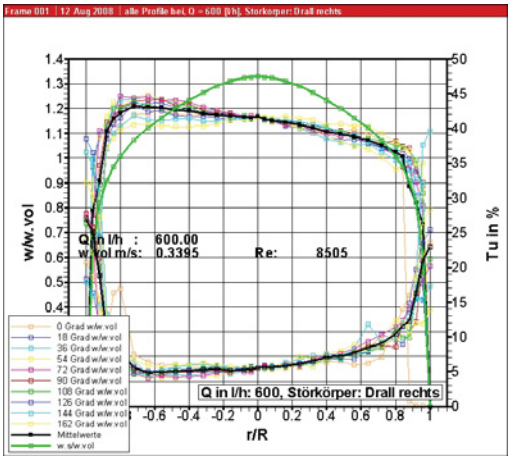

Figure 7: Normalized velocity profiles along the 10 diameters of the measuring grid and their average (black line) compared with the theoretical velocity profile of a fully developed turbulent flow (green line); Pipe diameter d=25 mm, distance between swirl generator and measuring section 5 d, flowrate 600 l/h

3. MEASURING PROGRAMMES AND EXPERIMENTAL GOALS

Using the LDA techniques described, velocity distributions in liquid flows have been determined for a wide field of conditions, for instance:

- At flowrates between 60 l/h and 120 m^3/h
- In pipes with diameters between 5 and 300 mm
- At temperatures between 10 °C and 50 °C
- Under „ideal“ undisturbed flow conditions (after straight pipes of various lengths)
- Behind diverse disturbing pipe elements (elbows, constrictions, diffusors), standard disturbers (swirl generators, diaphragms, plates partly blocking the pipe cross section), and flow straighteners or conditioners (perforated plates, meshes etc.)

In most of the cases, these flow measurements had been made in connection with investigations of certain flow meter types the metrological behaviour of which was expected to be affected by the respective velocity distribution at their inlet. Therefore error curves of these flow meters had been determined under exactly the same “disturbed” flow conditions as used for the LDA investigations. Particular interest was directed to find out a systematic correlation between the concrete flow conditions and the corresponding changes in the meter’s indication – at first to reduce the necessary amount of further investigations because of the possibility to take advantage of similarity effects, and secondly to identify limits and parameter fields where the flow disturbances do not significantly affect the flow meter behavior.

However, for this purpose the graphical presentations of Fig. 4 to Fig. 7 are not entirely sufficient – they are giving only *qualitative* pictures of the flow and the processes running inside. But the aim was to determine special parameters describing a certain flow *quantitatively*.

4. DEFINITION OF DIMENSIONLESS FLOW-CHARAKTERIZING PARAMETERS

Altogether, four dimensionless parameters have been determined to characterize completely each kind of a pipe flow [5, 6]. The axial velocity components are estimated by the following parameters:

- the *profile factor* K_p comparing the shape of the profile measured $K_{p,meas}$ with the ideal profile $K_{p,s}$ of a fully developed laminar or turbulent flow (Fig. 8)

$$K_p = \frac{K_{p,meas}}{K_{p,s}} = \frac{\int (w_m - w)\,dr}{\int (w_{m,s} - w_s)\,dr} \qquad (1)$$

where w_m - velocity at the pipe centre r/R=0
w - local velocity at r/R
index ,s - in relation to the ideal (“standard”) profile

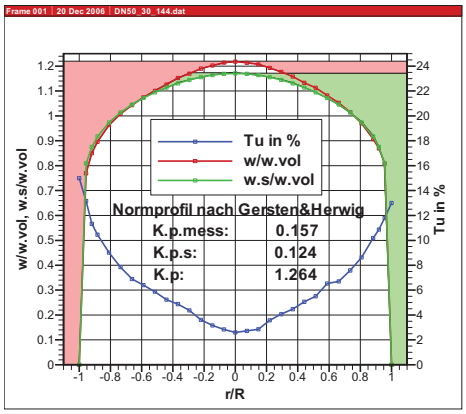

Figure 8: Graphical explanation of the profile factor K_p in accordance with equation (1)

The profile factor gives information about the flatness (K_p<1) or peakedness (K_p>1) of the profile. In the case of a fully developed flow, the profile factor takes the value 1. The ideal ("standard") profiles were:

- the HAGEN-POISEUILLE profile for laminar flows and
- the GERSTEN&HERWIG profile [see 7, 8] for turbulent flows.

- the *asymmetry factor* K_a representing the displacement of the center of area away from the rotation symmetry line (Fig. 9)

$$K_a = \frac{\int_0^1 r \cdot w \cdot \mathrm{d}\left(\frac{r}{R}\right)}{2 \cdot R \cdot \int_0^1 w \cdot \mathrm{d}\left(\frac{r}{R}\right)} \quad \text{in \%} \qquad (2)$$

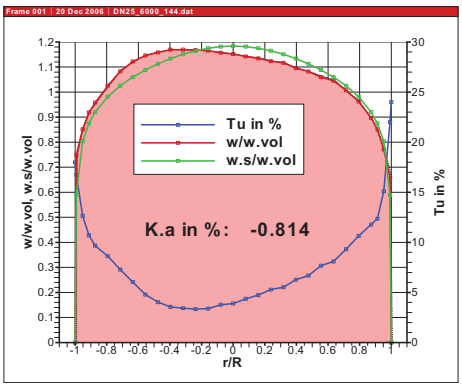

Figure 9: Graphical interpretation of the asymmetry factor K_a in accordance with equation (2)

- the *turbulence factor* K_{tu} characterizing the velocity fluctuations of the flow to be investigated - Fig. 10 shows a typical velocity spectrum recorded by the LDA in a measuring point.

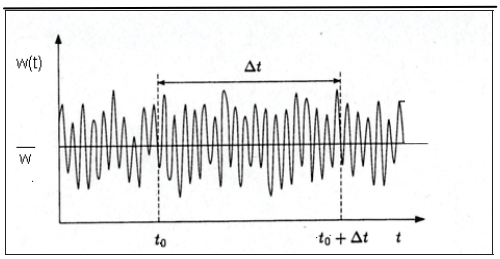

Figure 10: Typical velocity spectrum of a pipe flow with a constant flowrate

The corresponding degree of turbulence *Tu* calculates according to

$$Tu = \frac{s}{\overline{w}} \quad \text{in \%} \qquad (3)$$

where $w(t)$ - current velocity
$\overline{w}$ - mean velocity over the time Δt
s - standard deviation of w=f(t)

The turbulence factor K_{tu} itself is defined as the ratio of the maximum degree of turbulence Tu_{max} within the core area of the flow between -0,2≤ r/R≤ 0,2 and the degree of turbulence of the corresponding fully developed flow Tu_s

$$K_{tu} = \frac{Tu_{max}\Big|_{r/R=-0,2}^{r/R=0,2}}{Tu_s} \qquad (4)$$

where in accordance with [9]

$$Tu_s = 0{,}13 \cdot \left[Re\left(\frac{w_m}{w_{vol}}\right) \right]_s^{\frac{1}{8}} \qquad (5)$$

Figure 11 demonstrates the given definitions graphically.

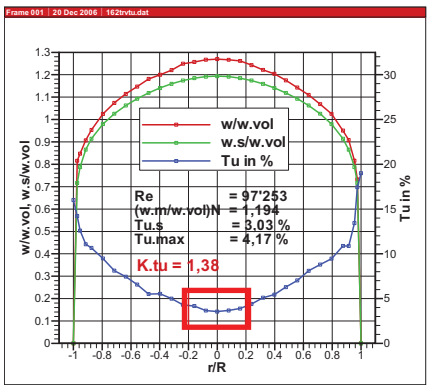

Figure 11: Explanation of the turbulence factor K_{tu} in accordance with equations (4) and (5)

Beside these three flow-characterizing parameters basing upon the axial velocity components of the flow, a further parameter was defined using information from the tangential velocity components

- the *swirl angle* Φ (Fig. 12)

$$\Phi = \arctan\left(\frac{v}{w_{vol}}\right) \qquad (6)$$

where v - tangential component of the velocity vector in the measuring point observed

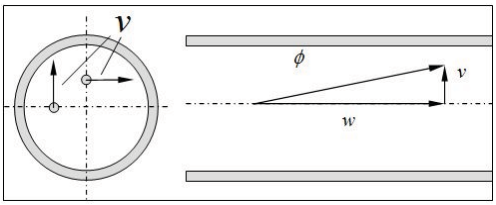

Figure 12: Graphical interpretation of the swirl angle

After defining these parameters and testing their suitability, corresponding automatic calculations were included into the data evaluation software of the LDA system. Now it was possible to get a great amount of comparable data for very different measuring situations (see chapter 3). Analyzing and discussing the results of more than hundred diverse flow measurements and considering the corresponding (situation-dependent) flow meter indications, concrete quantitative limits for the four flow parameters could be found.

Table 1: Acceptance criteria for the flow parameters

Profile factor K_p	Range	$0{,}8 \leq K_p \leq 1{,}3$
Asymmetry factor K_a	Maximum value	$K_a \leq 1\%$
Turbulence factor K_{tu}	Maximum value	$K_{tu} \leq 2$
Swirl angle Φ	Maximum value	$\Phi \leq 2°$

If flow parameters measured at the inlet section of a flow meter meet the acceptance criteria listed in table 1, it can be expected that the flow meter is not significantly affected by the incoming flow conditions. If only one parameter is not matching the criteria, measures should be taken to avoid possible changes in the meter behavior due to disturbances in the flow. The concrete values of the parameters give a good orientation about what could be done to improve the flow conditions, for example, by prolonging the straight pipe in front of the meter, or by inserting special flow conditioners or straighteners into the meter's inlet pipe.

5. EXTENSION OF THE FIELD OF APPLICATION TO MULTI-JET CARTRIDGE WATER METERS

In most of the cases, the study of the flow conditions within the pipe sections only *in front of a flow meter* does not yet completely explain the meter's reaction resulting in unpredictable unwanted changes of its indication. Consequently, the investigation had to be continued modifying the LDA system to gain access to the *internal flow areas of the meter* and to study directly the respective flow processes in dependence on the concrete flow meter construction.

Due to a current cause of interest, it was decided to start such investigations with a co-axial multi-jet water meter [10] consisting of a measuring cartridge attachable to the corresponding pipe section by screwing it into an appropriate meter body (see Fig. 13). This body remains in the pipe, i.e. it becomes part of the general domestic water installation for all the time. Necessary metrological and legal activities are limited to the cartridge - all tests and, in particular, the verifications are made not using the original body but only a specimen. The required replacing of a water meter after expiry of the verification date applies only to the cartridge. On the other hand, each body housing forms a part of the measuring volume and that way can exert noticeable influence on the measuring behavior of the meter. Because of the lack of any theoretical or experimental data, serious doubts had been expressed that a cartridge meter can be considered as a water meter in the sense of the new European Measuring Instruments Directive [11] – a real need for action arose.

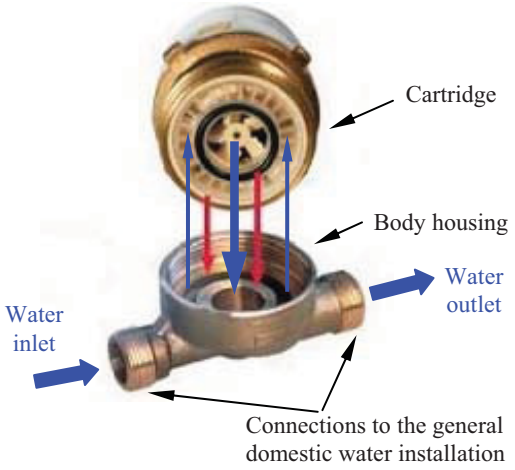

Figure 13: General principle of a multi-jet cartridge water meter

The most interesting area of investigation inside such a multi-jet cartridge water meter is the concentric ring gap where the horizontally incoming water changes its direction and enters vertically the cartridge.

To ensure optical access even to this region, the window chamber of the LDA system, as well as the water meter, had to be adapted to the new measuring situation. The cartridge was completely replaced by special glass tubes exactly simulating the real water flow through the cartridge (Fig. 14).

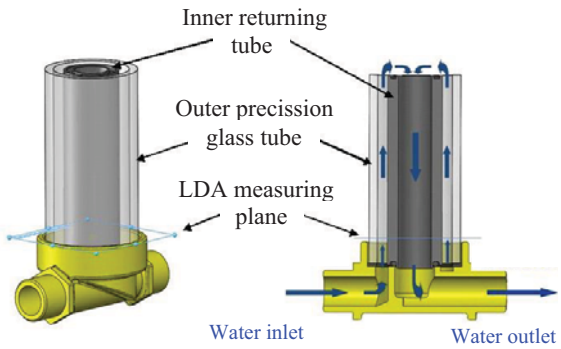

Figure 14: Modification of the multi-jet cartridge water meter to provide the optical access to the area of interest inside the meter

6. ADAPTION OF THE LDA SYSTEM

In addition to the modifications of the water meter, the window chamber as well as the software of the LDA system had also to be adapted. The upper cover of the window chamber has to hold a special flange which diverts the flow from the outer ring gap into the inner water meter outlet. Thus, the third measuring position is not practicable what requires an new solution for the window chamber. The adapted construction (Fig. 15) allows the optical access to the measuring area only by moving the LDA unit in the horizontal plane.

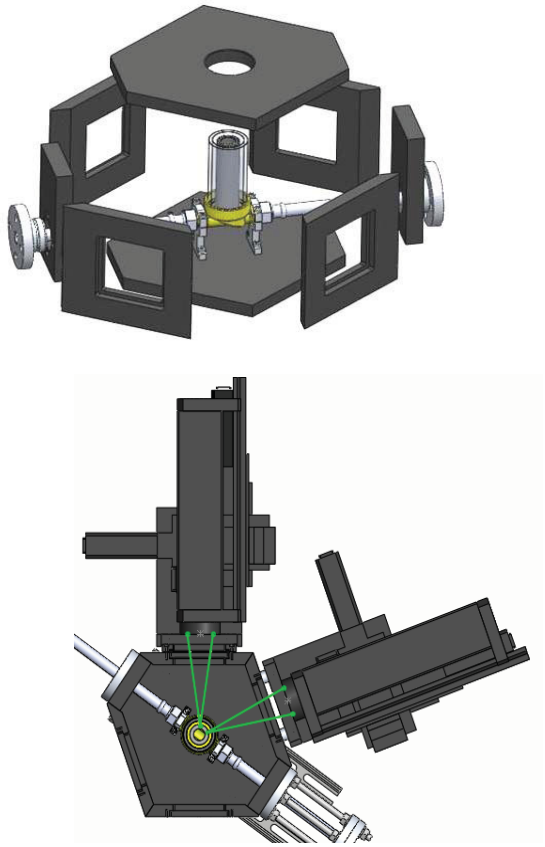

Figure 15: New construction of the window chamber allowing optical access to the LDA measuring plane inside the water meter according to Fig. 14

The measuring grid was also changed: six circles of 72 measuring points each (what corresponds to an angular distance of 5 °) are arranged inside the 6 mm ring gap (Fig. 16). So, altogether each velocity distribution consists of 432 single measuring points.

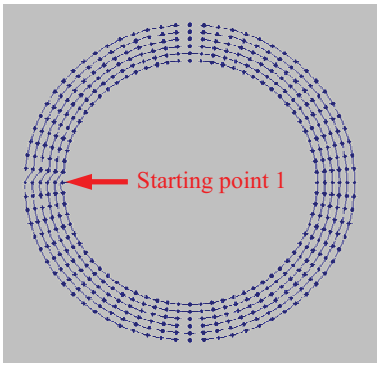

Figure 16: Measuring grid modified to measure velocity distributions inside the ring gap of a multi-jet cartridge water meter

The data processing and evaluation was modified as well. Fig. 17 shows an example of a distribution of the axial velocity component inside the ring gap (top view). Here, the incoming flow is completely unaffected by any disturbance. It enters the body housing horizontally from the left, splits and circulates through the lower ring channel, turns into the upright direction and moves now towards the observer (Fig. 18).

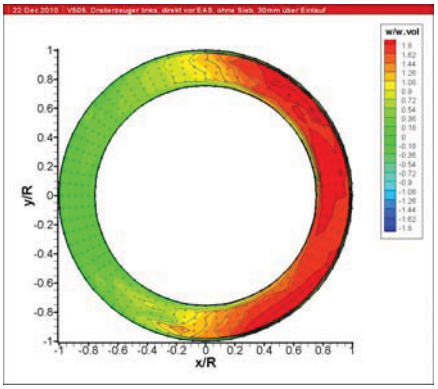

Figure 17: Distribution of the axial velocity component of an undisturbed incoming flow inside the ring gap of a multi-jet cartridge water meter for a flowrate of 600 l/h

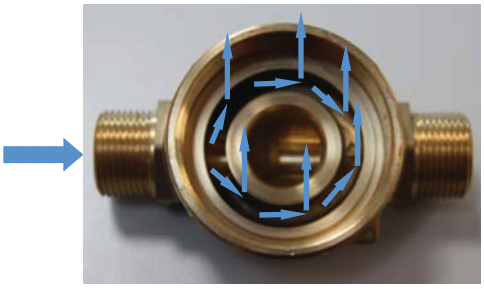

Figure 18: Demonstration of the flow behavior inside the ring gap

7. DEFINITION OF A FURTHER DIMENSIONLESS FLOW-CHARACTERIZING PARAMETER

Also in the case of the cartridge meter investigations, the LDA measurements have been made in a very wide range of different flow conditions and configurations what resulted in a great amount of qualitative descriptions of the corresponding velocity distributions in the form of Fig. 17 [1)] – and again the question arose how to make them intercomparable.

Due to the specific construction of the cartridge, a minimum effect on its functionality can be expected when the flow is relatively "even" and rotation-symmetrically arranged over the whole ring gap. In that case, the wheel inside the cartridge will be driven continuously and uniformly, and the indication of the water meter should be highly reproducible. Therefore the aim was to find a parameter characterizing such an "ideal" velocity distribution – the so-called "homogeneity factor".

Fig. 19 presents, for the first instance, the primary data of a complete scan consisting of $i = 1 \ldots 432$ axial velocity values which are listed in the order of their determination. The horizontal red line specifies the mean volumetric velocity w_{vol} – at a flowrate of 600 l/h it amounts to 0,227 m/s. Negative velocity values imply a reversing flow at the corresponding measuring points.

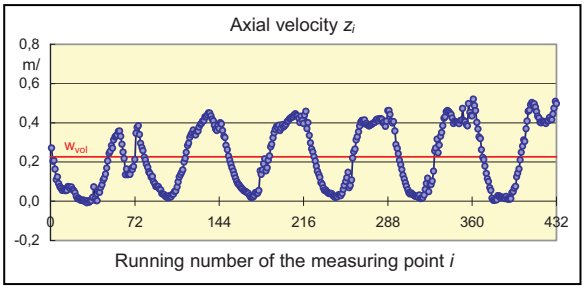

Figure 19: Axial velocity in m/s inside the ring gap in the order of their determination according to the given measuring grid at a flowrate of 600 l/h

Looking for a suitable definition of the homogeneity factor, the *quantity* of the flowing liquid will be of essential interest, but not its velocity. Therefore, an additional fact has to be taken into account: in dependence on the radial position of a measuring point, its velocity value will represent different portions of the total flow due to different sizes of the corresponding elemental areas. Consequently, each velocity value has to be multiplied by an appropriate weighing factor, increasing from inside to out. Moreover, a better impression about the active distribution of the flow across the ring gap will be reached looking at the mean values of the radial sectors around the gap. Fig. 20 shows the final diagram of the weighted normalized sectoral means $z_{mean;j}$ along each traverse inside the ring gap in dependence on their angular position j, starting at the water inlet on the left and moving anti-clockwise around the ring gap. In accordance with the given measuring grid (Fig. 16), the angular distance amounts to 5°.

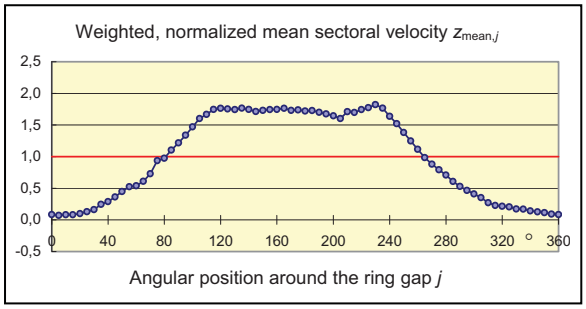

Figure 20: Weighted, normalized sectoral means of the axial velocity components along each of the 72 traverses inside the ring gap according to the values of Fig. 19

The wanted, preferably uniform flow distribution across the ring gap requires that the normalized means of Fig. 20 are as close as possible to the red line at $z_{mean} = 1$. Therefore the homogeneity factor F_h can be defined as

$$F_h = \frac{1}{72} \cdot \sum_{j=1}^{72} \left| z_{mean,j} - 1 \right| \qquad (7)$$

In the present example, F_h amounts to 0,63. In general, it can take a value between 0 and 1:

F_h=0 represents the case of a completely uniform flow distribution at the mean velocity level.

F_h=1 stands for an exactly 50% blockage of the ring gap (Fig. 21).

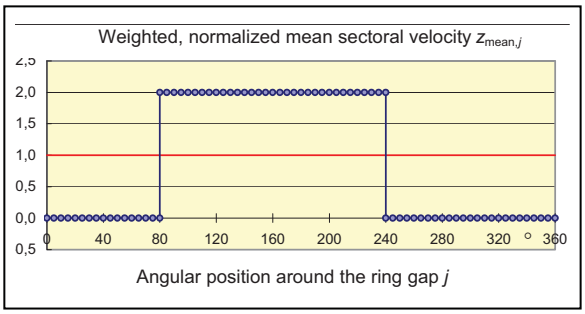

Figure 21: Weighted, normalized sectoral means of the axial velocity components along each of the 72 traverses inside the ring gap for the case of a complete 50% blockage of the ring gap

[1)] It could be shown that in the present case the analysis of the axial velocity components is quite enough for a comprehensible evaluation of the relationship between incoming flow conditions and the following water meter reaction

In real situations, the inlet of a cartridge is protected by using sieves of several designs (Fig. 22). Thus, each incoming flow has to pass these sieves before it moves upwards through the gap. Due to the standardized construction of the water meters [10], the sieves are normally positioned inside the lower part of the body still beneath the LDA measuring level.

Figure 22: Two types of the lower inlet part of different multi-jet cartridge water meters comprising corresponding sieves

The next Fig. 23 gives an example of a ring gap flow when a sieve is put into the lower part of the body. Such a configuration simulates the real case when a cartridge (Fig. 22) would be screwed in. The corresponding homogeneity factor amounts to 0,164.

The (in-)dependence of the such a gap flow on the flowrate can be demonstrated by the presentations of Fig. 24. The flowrates change between 30 l/h and 1200 l/h without any changes of the measuring installation. The diagrams look quite similar. The respective homogeneity factors amount to

0,229 at 60 l/h
0,206 at 300 l/h
0,245 at 600 l/h
0,247 at 1200 l/h.

Further investigations using another sieve design yielded a homogeneity factor of 0,231 at a flowrate of 600 l/h.

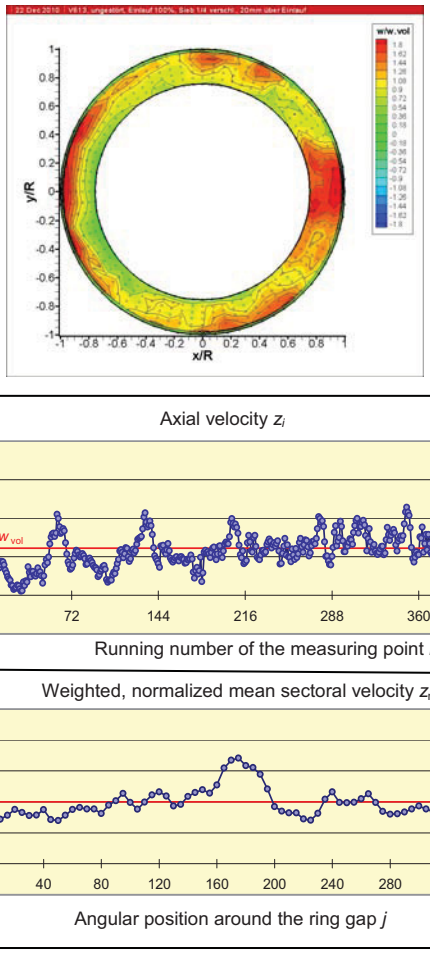

Figure 23: Axial velocity distribution and its numerical decomposition in accordance with Fig. 17, Fig. 19 and Fig. 20;
flowrate 600 l/h through a multi-jet cartridge water meter body equipped with a sieve

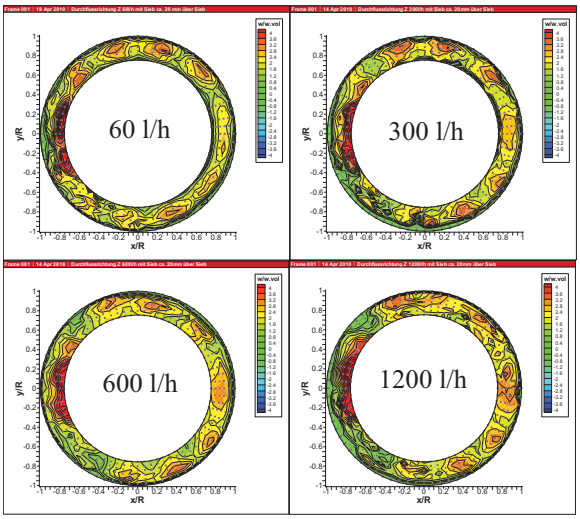

Figure 24: Axial velocity distributions in the ring gap of a multi-jet cartridge water meter after a sieve was put into the lower part of the meter body to simulate a real cartridge inlet;
flowrates between 60 l/h and 1200 l/h

Altogether, 33 different measuring arrangements of the 15 mm multi-jet cartridge water meters have been investigated:

- Under „ideal“ undisturbed flow conditions (after straight pipes of various lengths)
- Behind several disturbing pipe elements (elbows) and standard disturbers (swirl generators)
- Under conditions simulating strong contaminations and accumulated dirt and soil by sealing partly the sieves and inlet pipes up to 50 %.

For all these measuring situations, the corresponding error curves of the complete cartridge meters have been determined as well. So it was again possible to look for a correlation between the flow conditions in front of or inside the cartridge meter and its metrological behavior.

Interesting findings could be attained:

- The homogeneity factors K_h amount to
  - 0,1 … 0,3 for all configurations with a sieve and non-blocked meter inlet (but with disturbers and contaminated sieves)
  - 0,3 … 0,5 for all configurations with a sieve and a 50 % blocked meter inlet
  - 0,5 … 0,8 for all configurations without a sieve
- The error curves of the completed cartridge meters had been significantly affected only in one situation – in the case of absence of any sieves, i.e. when the homogeneity factor is greater than 0,5.

Because of the facts that all cartridge water meters possess protecting means at their inlet section, and that the dimensions of the “interface” between cartridge and body are internationally standardized [10], it can be expected that correctly installed and maintained multi-jet cartridge water meters can be treated as water meters in accordance with the European Directive MID [11].

8. ACKNOWLEDGEMENT

The author would like to thank Dr. Ulrich Müller (OPTOLUTION Inc. Switzerland) and Dr. Michael Dues (ILA Inc. Germany) for the permanent, highly competent support during each stage of applying and modifying the LDA unit. Thanks go as well to Andreas Hein, Torsten Jahn and Ulrich Jakubczyk for their careful, exact and diligent completion of the comprehensive experimental and technical work.

9. REFERENCES

[1] F. Adunka, “Installation effects at water and heat [1)]meters,” 2nd Middle-East conference 2004, Bahrain.

[2] G. Wendt, “Einfluss des Strömungsprofils auf das Messverhalten von Wasser- und Wärmezählern,“ PTB-Bericht PTB-MA-79, Braunschweig, Februar 2007, pp. 25-41.

[3] T. Lederer, G. Wendt, P.N. Matthies, H. Többen, U. Müller, M. Dues, „Verfahren zur Messung von Geschwindigkeitsverteilungen eines durch einen Rohrquerschnitt strömenden Fluids und Messanordnung zur Durchführung des Verfahrens,“ German Patent No. 10 2006 039 489.

[4] U. Müller, M. Dues, H. Baumann, „Vollflächige Erfassung von ungestörten und gestörten Geschwindigkeitsverteilungen in Rohrleitungen mittels Laser-Doppler-Velocimetrie,“ Technisches Messen 74 (2007), pp. 342-352.

[5] U. Müller, M. Dues, G. Wendt, J. Rose, H. Baumann, „Richtlinie zur strömungstechnischen Validierung von Kalibrier-Prüfständen im Rahmen der EN 1434,“ Hrsg. AG Laseroptische Strömungsmess-technik, PTB Berlin 2006.

[6] M. Dues, U. Müller, „Messtechnische Erfassung es Strömungsprofils – Kennzahlen zur Charakterisierung der Strömungsbedingungen,“ PTB-Bericht PTB-MA-79, Braunschweig, Februar 2007, pp. 43-74.

[7] K. Gersten, G. Herwig, „Strömungsmechanik. Grundlagen der Impuls-, Wärme- und Stoffübertragung aus asymptotischer Sicht“, Vieweg-Verlag, Braunschweig Wiesbaden 1992.

[8] K. Gersten, „Fully developed turbulent pipe flow,” In: W. Merzkirch, “Fluid mechanics of flow metering,” Springer-Verlag, Berlin Heidelberg New York 2005.

[9] F. Durst, M. Fischer, J. Jovanovic, H. Kikura, „Methods to set up and investigate low Reynolds number, fully developed turbulent plane channel flows,” J. Fluids Eng., 120 (1998), pp. 496-503.

[10] European Standard EN 14154: 2005 + A1:2007 “Water meters”.

[11] European Directive 2004/22/EC (Measuring Instruments Directive MID).